Longqiu Shao ✉
Qinghua Zhang
Gaowei Lei
Naiquan Su
Penghui Yuan

https://doi.org/10.21278/TOF.463033721
ISSN 1333-1124
eISSN 1849-1391

AN IMMUNE DETECTOR-BASED METHOD FOR THE DIAGNOSIS OF COMPOUND FAULTS IN A PETROCHEMICAL PLANT

Summary

Aiming at the serious overlap of traditional dimensionless indices in the diagnosis of compound faults in petrochemical plants, we use genetic programming to construct optimal indices for that purpose. In order to solve the problem of losing some useful fault feature information due to classification processing, during the generation of the dimensionless index immune detector, such as reduction and clustering, we propose an integrated diagnosis method using each dimensionless index immune detector. Simulation results show that this method has high diagnostic accuracy.

Key words: *petrochemical plant, dimensionless index, immune detector, compound fault, integrated diagnosis*

1. Introduction

With the rapid development of petrochemical industry, petrochemical plants are becoming larger and more complicated. Due to the complexity of the structure and the processes of these plants, multiple compound faults often occur. When this happens, different fault characteristic signals are mixed with each other, which presents complex symptoms such as complex coupling and fuzziness; this often makes various diagnosis methods based on the frequency-domain analysis as the basic technology helpless [1-3]. Therefore, compound fault diagnosis is a difficult problem in the field of fault diagnosis in petrochemical plants [4-6]; this is especially true in the research on integrated diagnosis methods with the focus on accuracy and real-time performance [7-14].

In complex environments, vibration monitoring signals of petrochemical plants often contain a large number of nonlinear and random information, which causes great difficulties in the analysis of fault signals [7, 15]. Considering that vibration time-domain signals are the most basic and original signals, it would be very beneficial to maintain their basic features. For fault diagnosis, it is of major importance that fault features can be directly extracted from such time-domain signals [15]. In the time-domain analysis, the probability density function of vibration signals can better reflect the fault information., Dimensional indices, such as mean value and root mean square value, and dimensionless indices in the amplitude domain, such as waveform index, margin index, and pulse index, have been derived through the probability density function of vibration signals [16]. In practice, although the dimensional index is sensitive to fault characteristics and its value will rise with the development of faults, it will also change due to a change in the operating conditions (such as load and rotational speed), it is easily affected by interference, and its performance is not stable enough. In contrast, the dimensionless index is insensitive to the disturbance in the vibration monitoring signal, and its performance is relatively stable. In particular, the dimensionless indicators are insensitive to changes in the amplitude and frequency of the signal, i.e. they have little to do with the operating conditions of the machine. Consequently, the dimensionless index has been widely used in the fault diagnosis of petrochemical plants [17]. Among the dimensionless indices, the kurtosis index and the pulse index are more sensitive to the impact fault, especially in the early stage of the fault; in the case of the impact fault, the high value of the pulse is reduced, and the values of other indices do not increase much, but the values of the kurtosis and the pulse index increase more sharply [18]. Therefore, these two indices are more sensitive to the early failure of the petrochemical plant. However, in the actual operating conditions, the failure of the petrochemical plant is usually caused by a compound fault, that is, the fault of the equipment is a result of multiple single concurrent faults. The statistical data show that 80% of the faults in large petrochemical plants are complex and concurrent. The main difficulties are: (1) how to determine a corresponding range of dimensionless indices in the complex petrochemical environment; (2) how to distinguish between the dimensionless index ranges of equipment in proper working order and the dimensionless index ranges of faulty equipment since there is some overlapping between the fault ranges corresponding to each dimensionless index calculated using vibration monitoring data. This results in the uncertainty of diagnosis results. The above two difficulties greatly increase the complexity and difficulty of applying existing fault diagnosis methods.

Based on the above analysis, first, we use genetic programming to construct a new dimensionless index, we take genetic programming as an intelligent hierarchical structure optimization algorithm, we take the existing dimensionless index as the initial parameter and form a new composite parameter through the recombination and optimization of the original parameter. Secondly, in order to solve the problem of some useful fault feature information being lost due to classification processing, such as reduction and clustering, during the generation of the dimensionless index immune detector, we adopt an integrated diagnosis method using each dimensionless index immune detector. Simulation results show that this method has high diagnostic accuracy.

2. Compound Fault Diagnosis Model

A compound fault diagnosis model to be used in petrochemical plants, which is based on an immune detector, is shown in Fig. 1. In the process of diagnosis, the traditional dimensionless indices are recombined and optimized by genetic programming to construct new dimensionless indices, with the aim of overcoming the shortcomings of traditional dimensionless indices in the classification of faults in petrochemical plants. The classification effect is taken as a criterion for judging whether the new dimensionless index is good or bad. Finally, through this method, we obtain the index with the best classification ability; this index is used in the diagnosis of compound faults in petrochemical plants. Then, a variety of dimensionless immune detectors are defined based on the diversity principle of artificial immune system. Excellent detector sets that can be mapped to a unique fault feature space one by one are formed. Multiple dimensionless immune detectors are used for diagnosis at the same time. Cross detection of different detectors is used to increase the amount of available information, and finally integrated diagnosis is carried out to obtain the final diagnosis result.

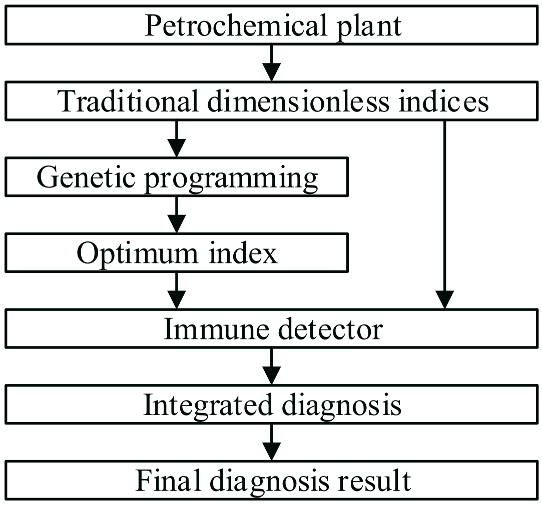

Fig. 1 An immune detector-based model for the diagnosis of compound faults in petrochemical plants

3. The Principle of Genetic Programming

The basic idea of genetic programming is based on the theory of biological evolution and the principle of heredity. An initial population suitable for a given problem is randomly generated, and the genotype of each individual in the population is represented as a tree. The adaptive value of each individual is calculated. According to the principle of survival of the fittest, genetic operators (replication, crossover and mutation, etc.) are selected for continuous iterative optimization of the population until the optimal solution or approximate optimal solution is found in a certain generation [19].

The function set, terminating character set, control parameter, fitness function, and the evolution terminating criterion should be determined when genetic programming is applied to solve problems. The details are as follows:

(1) Selection of the function set and the terminating set. After mathematical operations, such as addition, subtraction, multiplication, and division, performed among dimensionless indices, the obtained indices are still dimensionless. In this paper, six basic mathematical operations, including addition, subtraction, multiplication, division, extraction of the square root and squaring, are selected as function sets. Five traditional dimensionless indices, i.e. the waveform index, pulse index, margin index, peak index, and the kurtosis index) were selected as the terminating set.

(2) Selection of a control parameter. Population size refers to the total number of individuals contained in each generation of population. There is no definite method for selecting the population size. It is generally evaluated empirically and then modified according to the effect of system operation, which is 100 in this paper. Choosing an appropriate number of iterations can shorten the processing time without affecting the running effect too much. The maximum number of iterations depends on the size of the problem and can be determined by experiment. In this paper, the number of iterations is 100. Individual scale is the number of nodes that make up an individual. For more complex objects identified, more nodes must be used to describe them. However, for simple expressions, using larger individuals not only wastes computer resources, but may also make the form of the solution too complicated. In this paper, the maximum size of individuals is six. The basic operations of genetic programming include replication, crossover, and mutation. In general, the above operations are performed randomly on the basis of fitness, i.e. the greater the fitness

of an individual, the greater the probability that it will be selected. The selection method of fitness is a roulette selection method. According to the importance of these operations in genetic programming, the probability of replication is 0.2, the probability of crossover is 0.7, and the probability of mutation is 0.1.

(3) Design of fitness function. Fitness function is the basis of evolution and the driving force of natural selection, mainly to ensure the survival of the fittest. In the feature extraction of fault diagnosis, the idea of the Fisher information criterion can be used to make the classification effect achieve large between-class and small within-class scatters. In this paper, the fitness function is taken as follows:

$$F(v) = \frac{\min(D_{ij})}{D_\xi} \tag{1}$$

In the formula, D_{ij} represents the class spacing between classes *i* and *j*. The numerator represents the minimum value of between-class scatter, and the denominator represents the average value of within-class scatter. In the evolutionary calculation of genetic programming, the individuals with the highest fitness are selected; this ensures the classification ability of the optimal feature index to make the between-class scatter large and the within-class scatter small.

(4) Evolution terminating criterion. There are two criteria for termination:

1) The maximum fitness value of two adjacent generations did not change much, i.e.

$$\left|M_{i+1} - M_i\right| \le \delta \tag{2}$$

In the formula, M_i is the maximum fitness value of generation i, M_{i+1} is the maximum fitness value of generation (i+1), and δ is a predetermined minimum value.

2) Evolution to a pre-specified maximum evolutionary algebra, which is specified as 100 in this paper.

4. Generation of Immune Detector

The new improved negative selection algorithm [20,21] proposes two types of detector mutation search methods. In the first one, the detector is generated by using the mutation in its own space string according to a certain rule. In the second one, the mechanism of vaccination and the cloning selection are used to generate the detector directly in the fault space string according to certain rules. The two methods can not only generate the detector efficiently, but can also make the detector set fully contain the information of the fault space. The off-line training process of each dimensionless index immune detector is shown in Fig. 2. The immune detectors include initial detectors, maturity detectors, and excellent detectors, defined below:

(1) Initial detector. In this paper, the genetic variation mechanism is used to search the variation in the normal state space and the fault space of the equipment to generate a string equal to the length of the pattern as the initial detector.

(2) Maturity detector. The initial detector population has matured in the negative selection mechanism by matching with all pattern strings according to certain matching rules (such as r-continuous bits and the Hamming rule).

(3) Excellent detector. The maturity detector is matched with all the pattern strings with individual faults, and a unique fault detector that can correspond to various faults is generated. Then the excellent detector that can directly match various unique faults is extracted through reduction.

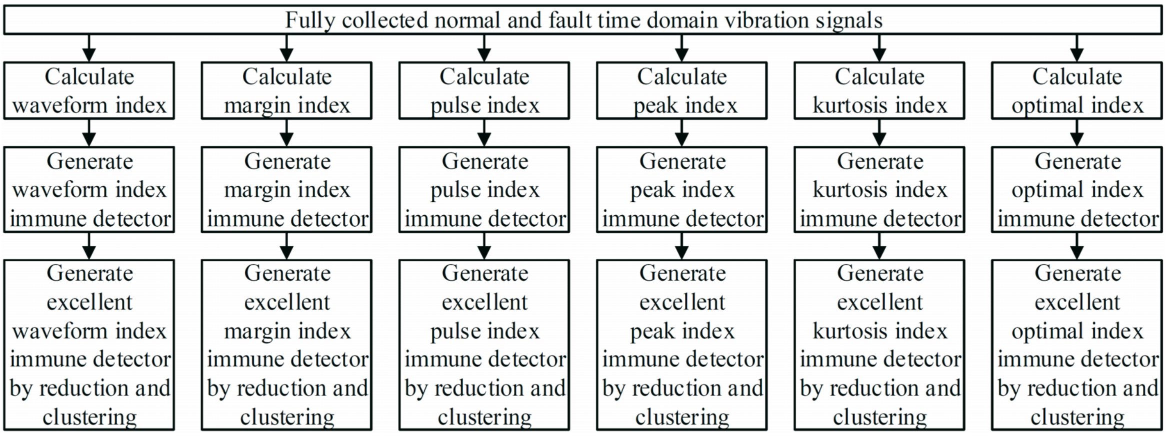

Fig. 2 A flowchart of each non-dimensional parameter offline training

5. Integrated Diagnosis

The dimensionless index immune detectors with separate fault diagnosis capabilities are designed to detect faults with unique characteristics. The sensitivity factor of the i type dimensionless index immune detector with a different sensitivity degree from that of the j type fault is set as m_{ij}, where $m_{ij}\leq 1$, i=1,2,...,l, j=1,2,...,n. The value of m_{ij} should be determined by comparing the ratio between the maximum value of a fault index and the minimum value of a normal index among dimensionless indices. The larger the ratio is, the more sensitive to faults the dimensionless index is, and the larger m_{ij} is; the smaller the ratio is, the smaller m_{ij} is. Furthermore, the degree to which the dimensionless index immune detector of type i preserves the useful feature information lost in the classification processing of type j by reducing and clustering is set as the useful fault information factor g_{ij}, where $g_{ij}\leq 1$, i=1,2,...,l, j=1,2,...,n. The value of g_{ij} should be determined by comparing the interval of lost information. The less lost information there is, the larger g_{ij} is; the more lost information there is, the smaller g_{ij} is. Finally, the relative diagnostic ability factor of the i type dimensionless immune detector for the j type fault is set as d_{ij}, where $d_{ij}\leq 1$, i=1,2,...,l, j=1,2,...,n. The values of d_{ij} are as follows:

$$d_{ij}=\frac{m_{ij}g_{ij}}{\sum_{k=1}^{l}m_{kj}g_{kj}} \tag{3}$$

The result of integrated diagnosis is expressed as:

$$F_j=\sum_{i=1}^{l}d_{ij}f_{ij},\ j=1,2,\cdots n \tag{4}$$

where, f_{ij} represents the j type fault detected by the i type dimensionless index immune detector. If the fault exists, f_{ij}=1, if not, f_{ij}=0.

Rules: when $F_j\geq\theta$, the j type fault is determined to occur and exist, where θ is the threshold value, and generally θ≥0.8.

6. Case Study

The experimental data in this paper comes from the petrochemical plant simulation test device of Guangdong Petrochemical Equipment Fault Diagnosis Key Laboratory. The petrochemical plant is composed of a motor, a gearbox, and a compressor. The support mode is simple, and the load is an 11kW five-stage centrifugal fan, as shown in Fig. 3. The common single fault or compound faults of petrochemical plants are simulated by replacing various faulty gears, bearings, transmission shafts, and other components.

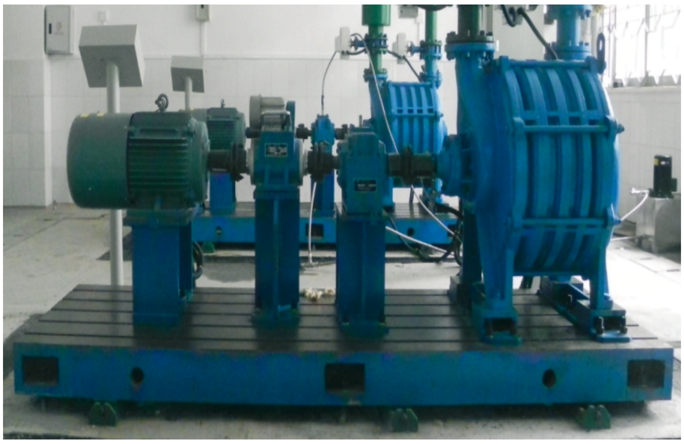

Fig. 3 The petrochemical plant simulation test device of Guangdong Petrochemical Equipment Fault Diagnosis Key Laboratory

EMT390 is used to obtain 100 data sets of waveform index (S_f), margin index (CL_f), pulse index (I_f), peak index (C_f), and kurtosis index (K_v) of the plant operating in normal conditions and in conditions with various faults of the equipment (cracked shaft, grinding gears, ball crack, cracked shaft + grinding gears, cracked shaft + ball crack, grinding gears + ball crack, and cracked shaft + grinding gears + ball crack). After the genetic programming optimization, an optimization index is obtained:

$$N_1 = K_v^2 + C_f^2 - CL_f I_f \tag{5}$$

Figure 4 shows the identification effect of the kurtosis index on the eight operating states defined above. Figure 5 shows the identification effect of optimal index N_1 on the eight operating states. The states are represented by the following signs: "○" represents the normal state, "×" represents the cracked shaft state, "+" represents the grinding gears state, "*" represents the ball crack state, "△" represents the cracked shaft + the grinding gears state, "□" represents the cracked shaft + the ball crack state, "◇" represents the grinding gears + the ball crack state, "☆" represents the cracked shaft + the grinding gears + the ball crack state (according to the order of sampling points). It can be seen from the figures that the kurtosis index cannot accurately identify the eight operating states, while the optimal index N_1 can clearly identify them.

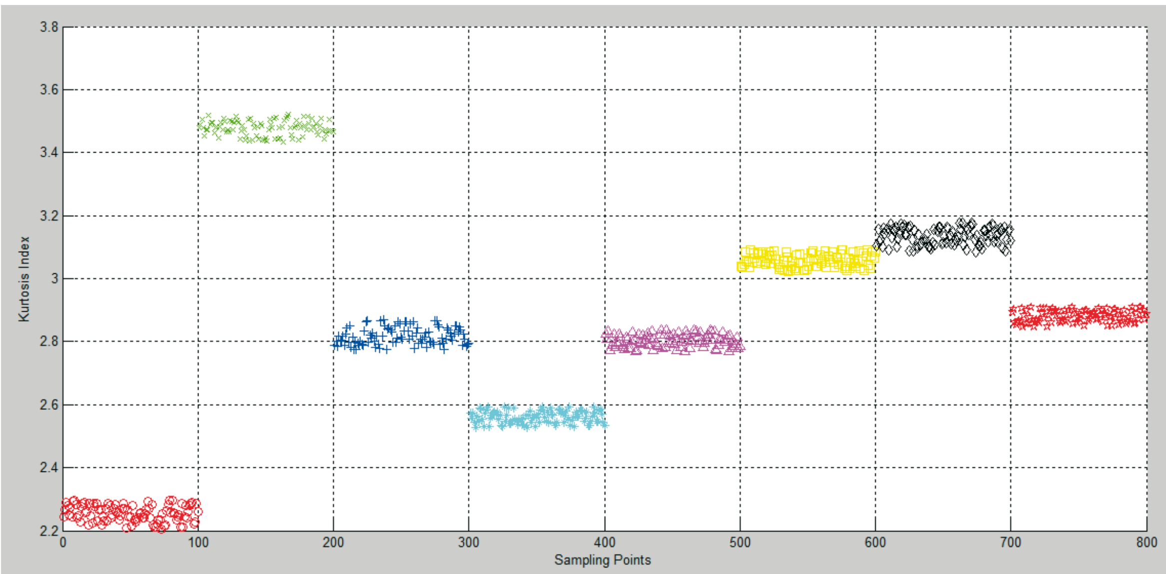

Fig. 4 The identification effect of the kurtosis index on the eight operating states

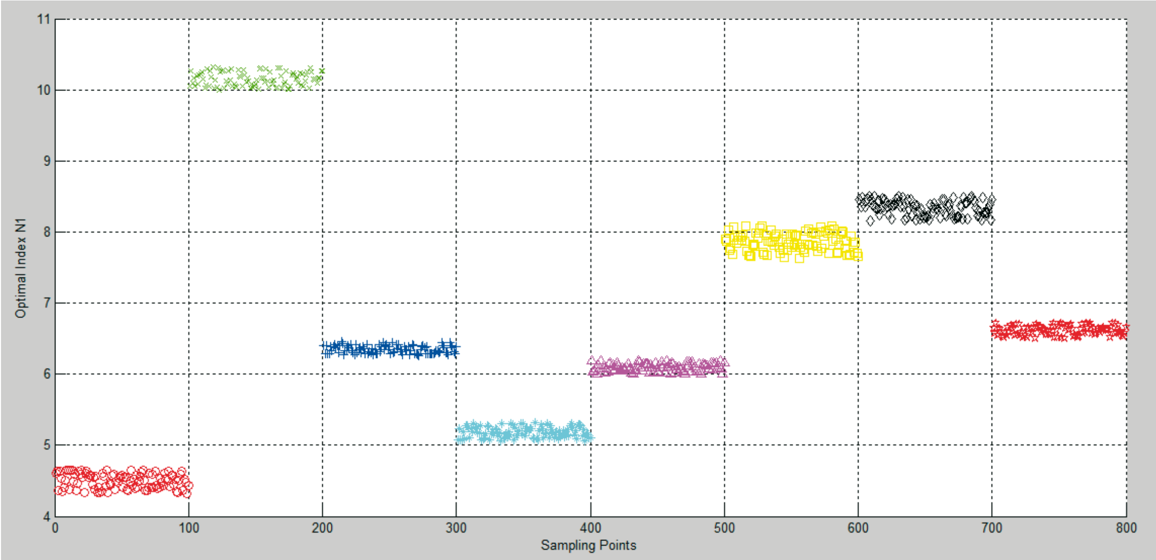

Fig. 5 The identification effect of the optimal index N_1 on the eight operating states

In order to verify the diagnostic effect of the optimal index N_1 on the compound fault, additional 100 data sets were selected for verification; a 95% confidence interval of the optimal index N_1 was used as the test standard. Table 1 shows the results obtained in the verification, where the percentage of the recognition ratio is within the confidence interval. As can be seen from Table 1, the results of verification are satisfactory.

Table 1 The recognition ratio of optimal index N_1

FAULT TYPE OF PETROCHEMICAL SIMULATION PLANT	ESTIMATE OF OPTIMAL INDEX N_1	CONFIDENCE INTERVAL	RECOGNITION RATIO (%)
NORMAL	3.632	[3.459, 3.805]	99
CRACKED SHAFT	10.422	[9.987, 10.857]	97
GRINDING GEARS	6.557	[6.296, 6.818]	96
BALL CRACK	5.295	[5.054, 5.536]	96
CRACKED SHAFT + GRINDING GEARS	6.013	[5.745, 6.281]	93
CRACKED SHAFT + BALL CRACK	7.766	[7.451, 8.081]	95
GRINDING GEARS + BALL CRACK	8.289	[8.088, 8.49]	92
CRACKED SHAFT + GRINDING GEARS + BALL CRACK	7.106	[6.903, 7.309]	90

The five dimensionless index values of the normal and various fault states of the plant are obtained, and then the value of the optimal index N_1 is calculated according to formula (5). The minimum and maximum values of each index are used as the value range of this index, as shown in Table 2.

Table 2 The value range of every dimensionless index

FAULT TYPE OF PETROCHEMICAL SIMULATION PLANT	S_F	C_F	I_F	CL_F	K_V	N_1
NORMAL	1.215	0.917	1.213	1.135	2.205	4.317
	1.227	0.931	1.232	1.186	2.297	4.663
CRACKED SHAFT	1.318	1.263	2.023	1.699	3.434	9.997
	1.342	1.285	2.059	1.747	3.521	10.328
GRINDING GEARS	1.242	1.320	1.923	1.657	2.776	6.262
	1.257	1.341	1.962	1.676	2.872	6.459
BALL CRACK	1.231	1.292	1.862	1.604	2.528	5.062
	1.246	1.311	1.897	1.651	2.593	5.315
CRACKED SHAFT + GRINDING GEARS	1.267	1.308	1.971	1.686	2.767	5.993
	1.283	1.319	1.986	1.702	2.836	6.191
CRACKED SHAFT + BALL CRACK	1.287	1.253	1.906	1.602	3.024	7.624
	1.304	1.267	1.927	1.642	3.092	8.092
GRINDING GEARS + BALL CRACK	1.302	1.286	1.957	1.659	3.085	8.162
	1.322	1.301	1.979	1.697	3.178	8.504
CRACKED SHAFT + GRINDING GEARS + BALL CRACK	1.258	1.337	2.003	1.745	2.845	6.504
	1.274	1.351	2.042	1.757	2.909	6.717

As can be seen from Table 2, except for the optimal index N_1, which has a good classification effect, the values of the other five traditional dimensionless indices corresponding to different faults exhibit a crossover and repetition phenomenon, and the unique characteristic values of each fault can only be obtained through the classification processing. The kurtosis index is taken as an example to illustrate the classification process. The known characteristic values of each fault are:

(1) Cracked shaft: 3.434 (C_{min})~ 3.521 (C_{max});

(2) Grinding gears: 2.776 (G_{min})~ 2.872 (G_{max});

(3) Ball crack: 2.528 (B_{min})~ 2.593 (B_{max});

(4) Cracked shaft + Grinding gears: 2.767 (CGM_{min})~ 2.836 (CG_{max});

(5) Cracked shaft + Ball crack: 3.024 (CB_{min})~ 3.092 (CB_{max});

(6) Grinding gears + Ball crack: 3.085 (GB_{min})~ 3.178 (GB_{max});

(7) Cracked shaft + Grinding gears + Ball crack: 2.845 (CGB_{min})~ 2.909 (CGB_{max}).

There is $B_{min}<B_{max}<CG_{min}<G_{min}<CG_{max}<G_{max}<CGB_{max}<CB_{min}<GB_{min}<CB_{max}<GB_{max}<C_{min}<C_{max}$, in this order:

(1) Ball crack + Crack shaft: 2.528 (B_{min})~ 2.593 (B_{max});

(2) Cracked shaft + Grinding gears: 2.767 (CGM_{min})~ 2.776 (G_{min});

(3) Grinding gears: 2.836 (CG_{max})~ 2.845 (CGB_{min});

(4) Cracked shaft + Grinding gears + Ball crack: 2.872 (G_{max})~ 2.909 (CGB_{max});

(5) Cracked shaft + Ball crack: 3.024 (CB_{min})~ 3.085 (GB_{min});

(6) Grinding gears + Ball crack: 3.092 (CB_{max})~ 3.178 (GB_{max});

(7) Cracked shaft: 3.434 (C_{min})~ 3.521 (C_{max}).

The classification processing is complete.

The other four dimensionless indices are classified in the same way. After the processing of the dimensionless index, the unique characteristics of each fault are highlighted, see Table 3 for details. After classification, each fault obtains unique fault characteristics, but some information about the fault is lost. In addition, some of the unique fault features are even too small to make the diagnosis capability decline. Using the diversity principle of artificial immune system, a variety of dimensionless immune detectors are defined, as shown in Fig. 2. Multiple dimensionless index immune detectors are used for diagnosis at the same time, and the cross detection of different detectors is used to increase the amount of available information; finally, an integrated diagnosis is carried out.

Table 3 The value range of every dimensionless index after classification processing

FAULT TYPE OF PETROCHEMICAL SIMULATION PLANT	S_F	C_F	I_F	CL_F	K_V	N_1
NORMAL	1.215 1.227	0.917 0.931	1.213 1.232	1.135 1.186	2.205 2.297	4.317 4.663
CRACKED SHAFT	1.322 1.342	1.267 1.285	2.042 2.059	1.702 1.745	3.434 3.521	9.997 10.328
GRINDING GEARS	1.246 1.257	1.320 1.337	1.927 1.957	1.657 1.659	2.836 2.845	6.262 6.459
BALL CRACK	1.231 1.242	1.301 1.308	1.862 1.897	1.642 1.651	2.528 2.593	5.062 5.315
CRACKED SHAFT + GRINDING GEARS	1.274 1.283	1.311 1.319	1.979 1.986	1.697 1.699	2.767 2.776	5.993 6.191
CRACKED SHAFT + BALL CRACK	1.287 1.302	1.253 1.263	1.906 1.923	1.602 1.604	3.024 3.085	7.624 8.092
GRINDING GEARS + BALL CRACK	1.304 1.322	1.286 1.292	1.962 1.971	1.676 1.686	3.092 3.178	8.162 8.504
CRACKED SHAFT + GRINDING GEARS + BALL CRACK	1.258 1.267	1.341 1.351	2.003 2.023	1.747 1.757	2.872 2.909	6.504 6.717

In the simulation experiment, five types of dimensionless index immune detectors, except the optimal index N_1 immune detector, were used for integrated diagnosis. The relative diagnostic capability factors of each immune detector were calculated according to formula (3), as shown in Table 4. The simulation results are shown in Table 5.

Table 4 The relative diagnose ability factor values of five types of dimensionless immune detectors

FAULT TYPE OF PETROCHEMICAL SIMULATION PLANT	RELATIVE DIAGNOSTIC CAPABILITY FACTORS OF				
	WAVEFORM IMMUNE DETECTOR	PEAK IMMUNE DETECTOR	PULSE IMMUNE DETECTOR	MARGIN IMMUNE DETECTOR	KURTOSIS IMMUNE DETECTOR
CRACKED SHAFT	0.174	0.199	0.139	0.224	0.264
GRINDING GEARS	0.228	0.339	0.338	0.06	0.035
BALL CRACK	0.189	0.124	0.349	0.066	0.272
CRACKED SHAFT + GRINDING GEARS	0.232	0.357	0.268	0.076	0.067
CRACKED SHAFT + BALL CRACK	0.225	0.215	0.273	0.03	0.257
GRINDING GEARS + BALL CRACK	0.261	0.149	0.168	0.107	0.315
CRACKED SHAFT + GRINDING GEARS + BALL CRACK	0.143	0.234	0.192	0.266	0.165

Table 5 The result statistics of compound fault diagnosis by five types of dimensionless immune detectors

FAULT TYPE	CRACKED SHAFT	GRINDING GEARS	BALL CRACK	CRACKED SHAFT + GRINDING GEARS	CRACKED SHAFT + BALL CRACK	GRINDING GEARS + BALL CRACK	CRACKED SHAFT + GRINDING GEARS + BALL CRACK
DIAGNOSTIC ACCURACY	91.2%	93%	92.7%	87.5%	85.8%	88%	80.1%

Then, six dimensionless index immune detectors, including the optimal index N_1 immune detector, were used for integrated diagnosis. The relative diagnostic ability factors of each immune detector were calculated according to formula (3), as shown in Table 6. The simulation results are shown in Table 7.

Table 6 The relative diagnose ability factor value of six types of dimensionless immune detectors

FAULT TYPE OF PETROCHEMICAL SIMULATION PLANT	RELATIVE DIAGNOSTIC CAPABILITY FACTORS OF					
	WAVEFORM IMMUNE DETECTOR	PEAK IMMUNE DETECTOR	PULSE IMMUNE DETECTOR	MARGIN IMMUNE DETECTOR	KURTOSIS IMMUNE DETECTOR	N_1 IMMUNE DETECTOR
CRACKED SHAFT	0.135	0.154	0.108	0.173	0.204	0.226
GRINDING GEARS	0.156	0.23	0.23	0.041	0.024	0.319
BALL CRACK	0.14	0.09	0.26	0.049	0.201	0.26
CRACKED SHAFT + GRINDING GEARS	0.146	0.224	0.168	0.048	0.042	0.372
CRACKED SHAFT + BALL CRACK	0.166	0.158	0.202	0.022	0.19	0.262
GRINDING GEARS + BALL CRACK	0.185	0.105	0.119	0.075	0.223	0.293
CRACKED SHAFT + GRINDING GEARS + BALL CRACK	0.105	0.171	0.140	0.194	0.121	0.269

Table 7 The result statistics of compound fault diagnosis by six types of dimensionless immune detectors

FAULT TYPE	CRACKED SHAFT	GRINDING GEARS	BALL CRACK	CRACKED SHAFT + GRINDIN G GEARS	CRACKED SHAFT + BALL CRACK	GRINDING GEARS + BALL CRACK	CRACKED SHAFT + GRINDING GEARS + BALL CRACK
DIAGNOSTIC ACCURACY	96%	97.8%	96.7%	93.5%	95%	94.6%	90.3%

Table 5 and Table 7 show that: (1) integrated diagnosis has a high diagnostic accuracy rate for the detection of simulated state; (2) the optimal index N_1 obtained by genetic programming optimization has a good diagnostic capability for compound faults, such as cracked shaft + grinding gears, cracked shaft + ball crack, grinding gears + ball crack, and split cracked shaft + grinding gears + ball crack.

7. Conclusion

A compound fault diagnosis method based on immune detector is proposed for petrochemical plants. Based on genetic programming, an optimal index for the compound fault diagnosis of petrochemical plants was constructed, and an integrated diagnosis method was proposed to solve the problem of fault information loss after classification. The simulation results show that the proposed method has high diagnostic accuracy, which provides an effective method for the diagnosis of compound faults in petrochemical plants.

Acknowledgments

The research was partially supported by the Key Project of Natural Science Foundation of China (Grant No. 61933013) and the National Nature Science Foundation of China (Grant No. 62073090). The research described in this paper was also partially supported by the Natural Science Foundation of Guangdong (Grant No. 2019A1515010700 and Grant No. 2022A1515010599).

REFERENCES

[1] D. Tsai, S. Wu, and W. Chiu. Defect detection in solar modules using ICA basis images[J]. IEEE Trans. Ind. Informat.,9(1), 122-131, 2013. https://doi.org/10.1109/TII.2012.2209663

[2] D. Zhou, X. He, Z. Wang, G. Liu, Y. Ji. Leakage fault diagnosis for an Internet-based three-tank system: An experimental study [J]. IEEE Trans. Control Syst. Technol., 20(4): 857-870, 2012. https://doi.org/10.1109/TCST.2011.2154383

[3] F. Caccavale, A. Marino, G. Muscio, F. Pierri. Discrete-time framework for fault diagnosis in robotic manipulators[J]. IEEE Trans. Control Syst. Technol., 21(5): 1858-1873, 2013. https://doi.org/10.1109/TCST.2012.2212196

[4] Z. W. Gao, C. Cecati, S. X. Ding. A survey of fault diagnosis and fault tolerant techniques-Part II: fault diagnosis with knowledge-based and hybrid/active approaches [J]. IEEE transactions on industrial electronics, 62(6): 3768-3774, 2015. https://doi.org/10.1109/TIE.2015.2417501

[5] Y. Zhang, N. Yang, S. Li. Fault isolation of nonlinear processes based on fault direction and features[J]. IEEE Trans. Control Syst. Technol., 22(4): 1567-1572, 2014. https://doi.org/10.1109/TCST.2013.2283925

[6] Y. Shatnawi, M. Al-Khassaweneh. Fault diagnosis in internal combustion engines using extension neural network [J]. IEEE Trans. Ind. Electron., 61(3): 1434-1443, 2014. https://doi.org/10.1109/TIE.2013.2261033

[7] Z. W. Gao, C. Cecati, S. X. Ding. A survey of fault diagnosis and fault tolerant techniques-Part I: fault diagnosis with model-based and signal-based approaches [J]. IEEE transactions on industrial electronics, 62(6): 3757-3767, 2015. https://doi.org/10.1109/TIE.2015.2417501

[8] Z. Chen, F. Lin, C. Wang, L. Wang, and M. Xu. Active diagnosability of discrete event systems and its applications to battery fault diagnosis [J]. IEEE Trans. Control Syst. Technol., 22(5): 1892-1898, 2014. https://doi.org/10.1109/TCST.2013.2291069

[9] X. Zhang, L. Tang, J. Decastro. Robust fault diagnosis of aircraft engines: A nonlinear adaptive estimation-based approach [J]. IEEE Trans. Control Syst. Technol., 21(3): 861-868, 2013. https://doi.org/10.1109/TCST.2012.2187057

[10] M. Grbovic, W. Li, N. Subrahmanya, A. Usadi, S. Vucetic. Cold start approach for data-driven fault detection [J]. IEEE Trans. Ind. Informat., 9(4): 2264-2273, 2013. https://doi.org/10.1109/TII.2012.2231870

[11] M. Liu, X. Cao, P. Shi. Fault estimation and tolerant control for fuzzy stochastic systems [J]. IEEE Trans. Fuzzy Syst., 21(2): 221-229, 2012. https://doi.org/10.1109/TFUZZ.2012.2209432

[12] Chen Qiuan, Wei Haipeng, Rashid Muhammad, Cai Zhiqiang. Kernel extreme learning machine based hierarchical machine learning for multi-type and concurrent fault diagnosis [J]. Measurement, 2021, 184(184). https://doi.org/10.1016/j.measurement.2021.109923

[13] Yao, D., Liu, H., Yang, J. et al. Implementation of a novel algorithm of wheelset and axle box concurrent fault identification based on an efficient neural network with the attention mechanism. Journal of Intelligent Manufacturing 32, 729–743 (2021). https://doi.org/10.1007/s10845-020-01701-y

[14] Yong Zhang, Huanzhen Hu, Zhenxing Liu,Min Zhao,Lei Cheng.Concurrent fault diagnosis of modular multilevel converter with Kalman filter and optimized support vector machine[J]. Systems Science & Control Engineering, 2019, 7(3). https://doi.org/10.1080/21642583.2019.1650840

[15] J. B. Xiong, Q. H. Zhang, G. X. Sun, Z. P. Peng, Q. Liang. Fusion of the dimensionless parameters and filtering methods in rotating machinery fault diagnosis [J]. Journal of networks, 9(5): 1201-1207, 2014. https://doi.org/10.4304/jnw.9.5.1201-1207

[16] Q. H. Zhang, Q. Hu, G. X. Sun, X. S. Si, A. S. Qin. Concurrent fault diagnosis for rotating machinery based on vibration sensors [J]. International journal of distributed sensor networks. 75(8): 93-102, 2013. https://doi.org/10.1155/2013/472675

[17] X. Dai, Z. Gao. From model, signal to knowledge: A data-driven perspective of fault detection and diagnosis [J]. IEEE Trans. Ind. Informat, 9(4): 2226-2238, 2013. https://doi.org/10.1109/TII.2013.2243743

[18] X. S. Si, C. H. Hu, J. B. Yang. On the dynamic evidential reasoning approach for fault prediction [J]. Expert Systems with Applications, 38(5): 5061-5080, 2011. https://doi.org/10.1016/j.eswa.2010.09.144

[19] KOZA J R. Genetic programming: on the programming of computers by means of natural selection[M]. Cambridge: MIT Press, 1992.

[20] Q. H. Zhang, Y. Qian, B. G. Xu, et al. Negative-selection algorithm of mutation search in self space to train detector [J]. Computer Applications, 2007, 27(3): 627-629.

[21] Q. H. Zhang, Y. Qian, B. G. Xu, et al. Fault detection algorithm of mutation search in non - self space. Computer Engineering and Applications, 2007, 43(28): 92- 94.

Submitted: 21.8.2021

Accepted: 08.02.2022

Mr. Longqiu Shao*
Prof. Qinghua Zhang
Mr. Gaowei Lei
Mr. Naiquan Su
Mr. Penghui Yuan
School of Automation, Guangdong University of Petrochemical Technology
Maoming 525000, China
*Corresponding author:
845338290@qq.com